

Article

# Crystal Structure of *Shigella flexneri* SF173 Reveals a Dimeric Helical Bundle Conformation

Ji-Hun Kim <sup>1,†</sup>, Hyung-Sik Won <sup>2,†</sup>, Won-Su Yoon <sup>3,4,†</sup>, Seung-Hyeon Seok <sup>4</sup>, Bong-Jun Jung <sup>3,4</sup>,  
Seu-Na Lee <sup>2</sup>, Dae-Won Sim <sup>2</sup> and Min-Duk Seo <sup>3,4,\*</sup>

<sup>1</sup> College of Pharmacy, Chungbuk National University, Cheongju 28160, Chungbuk, Korea; nmrjhkim@chungbuk.ac.kr

<sup>2</sup> Department of Biotechnology, College of Biomedical and Health Science, Konkuk University, Chungbuk 27478, Korea; wonhs@kku.ac.kr (H.-S.W.); leesn1029@naver.com (S.-N.L.); konapapa@nate.com (D.-W.S.)

<sup>3</sup> Department of Molecular Science and Technology, Ajou University, Suwon 16499, Korea; lovemyclub@naver.com (W.-S.Y.); bjjung@koruspharm.co.kr (B.-J.J.)

<sup>4</sup> Research Institute of Pharmaceutical Sciences and Technology (RIPST), College of Pharmacy, Ajou University, Suwon 16499, Korea; hsbsh83@gmail.com

\* Correspondence: mdseo@ajou.ac.kr; Tel.: +82-31-219-3450

† These authors contributed equally to this work.

Received: 29 December 2017; Accepted: 12 February 2018; Published: 14 February 2018

**Abstract:** We report the crystal structure and bioinformatic analysis of SF173, a functionally uncharacterized protein from the human enteropathogenic bacteria *Shigella flexneri*. The structure shows a tightly interlinked dimer formed by adimeric core comprising  $\alpha 2$  and  $\alpha 3$  helices from both subunits and swapping the N-terminal  $\alpha 1$  helix of each monomer. Structural inspection and genomic analysis results suggest that the SF173 might play its putative function by binding to SF172, the partially overlapped upstream product in the operon. As YaeO (an SF172 orthologue) has been identified to be an inhibitor of the bacterial transcription terminator Rho protein, SF173 is suggested to be involved in the regulation of Rho-dependent transcription termination, by inhibiting the Rho protein binding to SF172/YaeO.

**Keywords:** *Shigella flexneri*; SF173; X-ray crystallography; helical bundle

## 1. Introduction

Structural genomics, which aims for functional identification of genes (genome) through structure-based analyses of the gene products (proteome), has the additional benefit of frequently leading to the discovery of novel drug target proteins [1,2]. Here, we report the structural analysis of SF173, one of the targets chosen for our laboratory-scale structural genomics approach to the human enteropathogenic bacterium *Shigella flexneri*.

*Shigella* microbes are gram-negative, facultative anaerobic and rod-shaped bacteria from the family *Enterobacteriaceae* [3]. They are also considered important human pathogens, causing bacillary dysentery or shigellosis, which shows a broad spectrum of clinical symptoms from short-lasting watery diarrhea to acute inflammatory bowel disease [3,4]. 125 million cases of endemic shigellosis occur every year in Asia, with a heavy toll on infants and children [5]. The genus *Shigella* can be grouped into four different species with distinct characteristics [6]: *S. dysenteriae* (also referred to as group A) with 15 serotypes, *S. flexneri* (group B) with 6 serotypes, *S. boydii* (group C) with 19 serotypes, and *S. sonnei* (group D) with 1 serotype. In particular, *S. flexneri* mainly accounts for the endemic diseases prevalent in developing countries; for example, over 50% of the more than 10 million shigellosis patients estimated per year are attributed to *S. flexneri* [7]. Due to this important relationship with human

diseases, *S. flexneri* has been extensively studied and the complete genome of the *S. flexneri* 5a strain M90T has been sequenced [8].

Although the World Health Organization has announced an anti-Shigella vaccine to be a priority, no such a vaccine has yet been made available, despite massive global efforts. Antibiotics have been considered alternatives for shigellosis treatment, but the appearance of antibiotic-resistant *S. flexneri* has been recently reported [9,10], raising an urgent need for novel antibiotics to treat the infection. In terms of novel antibiotic development, structural genomics can contribute to identification of a novel, unique drug target molecule via structure-function analysis of previously uncharacterized proteins [2,11]. In addition, detailed structural information obtained from structural genomics study enables us to quickly and efficiently discover novel agents by structure-based rational drug design for targeting the newly validated proteins [11]. In this context, we initiated a laboratory-scale structural genomics study on *S. flexneri*, which includes structure determination of many functionally uncharacterized proteins; SF173, the product of the SF5M90T\_173 gene of the *S. flexneri* 5a strain, was one of the target proteins of this study. This functionally uncharacterized protein has 66 amino acid residues in its polypeptide chain and shows no significant sequence homology to other functionally known proteins. In order to carry out structure-based functional identification of the protein, we previously crystallized it successfully [12]. Here, we present the crystal structure of SF173 at a 1.47 Å resolution. SF173 forms a homodimer with a four  $\alpha$ -helical bundle conformation, and the N-terminal  $\alpha$ 1 helices are swapped between the component monomers. Further bioinformatics analysis suggests that SF173 is likely involved in the regulation of Rho-specific transcription termination.

## 2. Materials and Methods

### 2.1. Protein Purification and SEC-MALS Analysis

The native SF173 was prepared through the protocol used in a previous study [12]. Briefly, the *SF173* gene was subcloned into pET-21a vector (Novagen). The recombinant protein, SF173, was overexpressed in *E. coli* expression system. The SF173 tagged with poly-histidine in the C-terminus was purified on a HisTrap FF column (GE Healthcare), followed by HiPrep DEAE FF anion-exchange column (GE Healthcare). Further purification was performed by size exclusion chromatography (HiLoad 16/60 Superdex 200 column, GE Healthcare) with the final buffer (20 mM Tris-HCl at pH 7.2, 350 mM NaCl, 0.2 mM TCEP). SeMet-labeled SF173 was overexpressed using the M9 minimal media containing selenomethionine (SeMet) and a mixture of five amino acids (Lys, Phe, Ile, Leu, and Val), and it was purified using the same protocol as the native SF173. The purified protein was concentrated to approximately 20 mg mL<sup>-1</sup> and used for crystallization. The oligomeric form of SF173 was studied using size-exclusion chromatography (SEC)-multiangle light scattering (MALS) analysis. Purified proteins in 20 mM Tris buffer containing 350 mM NaCl, 0.2 mM TCEP at pH 7.2 were loaded onto an SEC column (WTC-015S5, Wyatt Technologies, Goleta, CA, USA) preequilibrated with the same buffer at a flow rate of 0.5 ml min<sup>-1</sup> and connected to a MALS detector (DAWN HELEOS-II, Wyatt Technologies) and a differential refractive-index detector (Optilab T-Rex, Wyatt Technologies). The molecular weight was calculated from the elution data using ASTRA software (Wyatt Technologies).

### 2.2. Crystallization and Data Collection

Crystals suitable for crystallographic analysis for the native SF173 were grown in a buffer containing 800 mM succinic acid, pH 7.0 [12]. SeMet-labeled SF173 was crystallized by the sitting-drop vapor-diffusion method in 96-well sitting-drop crystallization plates (Axygen, Corning, NY, USA) at 293 K. Initial crystallization conditions were analyzed by the sparse-matrix method [13] using commercially available kits, including Index HT, PEG/Ion HT, Crystal Screen HT (Hampton Research, Aliso Viejo, CA, USA), and Wizard I, II, III, IV (Emerald Bio, Palo Alto, CA, USA). The proteins (0.5  $\mu$ L) were mixed with equal volumes of reservoir solution and equilibrated against 80  $\mu$ L reservoir solution.

After several days, tiny crystals were obtained in WIZARD1/2 NO. 64 (1000 mM sodium citrate tribasic, 100 mM CHES/sodium hydroxide, pH 7.5) and Crystal Screen HT NO. 56 (0.2 M ammonium dihydrogen phosphate, 0.1 M tris, 50% *v/v* MPD, pH 8.5). To obtain single crystals for X-ray diffraction, the initial crystallization conditions were optimized by varying the volume ratio of mixture of protein solution and reservoir solution using the sitting drop vapor diffusion method. Different volumes of the protein solution (0.7  $\mu\text{L}$ ) and reservoir solution (1  $\mu\text{L}$ ) were mixed and equilibrated against 80  $\mu\text{L}$  reservoir solution in a 96-well plate (Axygen). The crystals suitable for X-ray diffraction were obtained in the buffer containing 1000 mM sodium citrate tribasic, 100 mM CHES/sodium hydroxide, pH 7.5. Data were collected using an ADSC Q270 detector on the 7A SBI beamline at the Pohang Accelerator Laboratory (PAL) (Pohang, Republic of Korea) using  $1^\circ$  oscillations, with a crystal to detector distance of 220 mm and a synchrotron X-ray beam of wavelength 0.97935  $\text{\AA}$ . The crystal was exposed for 0.5 s per image. The data set for SeMet-labeled SF173 was collected to a resolution of 1.47  $\text{\AA}$ . The data sets were processed and scaled using HKL-2000 [14]. The crystals belonged to space group I23, with unit cell parameter  $a = b = c = 110.244 \text{ \AA}$  and  $\alpha = \beta = \gamma = 90^\circ$ .

### 2.3. Structure Determination and Refinement

The crystal structure of SeMet-labeled SF173 was initially determined via single-wavelength anomalous dispersion (SAD) phasing [15] using AutoSol [16] in the program suite Phenix [17]. Manual model building was carried out using the program WinCoot [18] and the model was refined with the Phenix program [17]. The SeMet-labeled SF173 structure was used as the template of molecular replacement to solve the structure of native SF173. The final model was obtained through repeated model building and refinement attempts. The statistical parameters for the data collection and structure refinement are listed in Table S1.

## 3. Results and Discussion

### 3.1. Structure Determination and Overall Fold

The crystal structure of SF173 from the *S. flexneri* M90T strain was solved using a selenomethionine-labeled (SeMet) protein with diffraction data collected at a high resolution of 1.47  $\text{\AA}$  [12]. The refinement statistics are summarized in Table S1, and the  $2F_o - F_c$  electron density map of SF173 is shown in Figure S1. The atomic coordinates have been deposited in the Protein Data Bank under accession code 5H1N. The high quality of the refined structure was validated by the fact that all residues of the model lie in the preferred region of the Ramachandran plot. The structure is defined as a symmetric dimer with each subunit consisting of three  $\alpha$  helices:  $\alpha 1$ , residues 6–17;  $\alpha 2$ , residues 26–38;  $\alpha 3$ , residues 45–60 (Figure 1a). A multiangle light scattering (MALS) experiment was conducted to confirm the dimeric structure of SF173 in solution. As shown in Figure 1b, the molecular weight of SF173 in the solution was calculated as 17.1 kDa, which indicates that SF173 forms a dimeric structure according to the theoretical monomeric molecular weight of 8.18 kDa. Overall, the dimeric structure was characterized as a helix-winged anti-parallel four-helix bundle fold. The C-terminal  $\alpha 2$  and  $\alpha 3$  from one monomer and  $\alpha 2'$  and  $\alpha 3'$  from the other monomer (henceforth, residues and helices in the opposite subunit are denoted with primed numbers) form the central, interchain four-helix bundle framework, while the N-terminal  $\alpha 1$  and  $\alpha 1$ - $\alpha 2$  loop are swapped between the monomers to surround the central scaffold (Figure 1a). This tight dimerization is stabilized by hydrophobic interactions between multiple non-polar residues from all  $\alpha$  helices. In particular, the C-terminal part of  $\alpha 3$  provides a helical core that is surrounded by three other helices,  $\alpha 2$ ,  $\alpha 1'$ , and  $\alpha 2'$ . Thus, the highly conserved poly-alanine region in  $\alpha 3$  (Figures 2a and S2), which is known to have a great propensity for building a hydrophobic packing core [19], appears to play a key role in maintaining this interesting architecture. In addition, four salt bridges (R11 to E49', R11' to E49, E36 to K50', and E36' to K50) and six hydrogen bonds (C5 to N35', C5' to N35, Y12 to E66', Y12' to E66, G21 to Y53', and G21' to Y53) between the monomers (Figure S3) also contribute to stabilization of the overall helical bundle conformation.

A structural similarity search using the DALI server [20] indicated that the SF173 structure can be regarded as a novel fold. The DALI outputs showed a significant ( $>5.0$ ) Z-score only for the top-ranked structure (PDB 3W3U, importin subunit beta-3; Z-score 5.5) with a small internal fraction being matched. Likewise, in the case of the other candidates for structural homologues with Z-scores over 4.0, including the oxyb protein (PDB 4TX3; Z-score 4.3), deoxyhypusine hydroxylase (PDB 4D4Z; Z-score 4.1), and GTP-binding nuclear protein Ran (PDB 1WA5; Z-score 4.1), fractional helices only match a small part of the core structure of SF173. As meaningful information could not be derived from the DALI search, we attempted to analogize the function of SF173 using other bioinformatic analyses as follows.

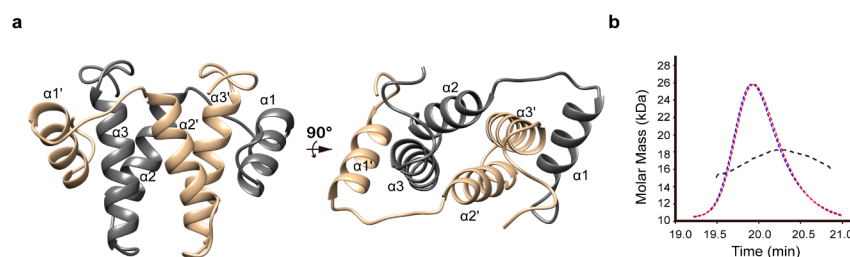


**Figure 1.** Structural description of SF173. (a) Ribbon presentation of the SF173 crystal structure. Individual polypeptide chains are shown in different colors (gold and gray); (b) Size exclusion chromatography (SEC) multi-angle light scattering (MALS) analysis of SF173. Elution profile was detected by MALS (red) and refractive index (RI; blue) and the calculated molar mass of SF173 is fitted by black dotted lines.

### 3.2. Structural Similarity to Colicin Immunity Proteins

Based on the InterPro web resource for protein sequence analysis and classification [21], SF173 belonged to an uncharacterized protein family, UPF0253, which is commonly expressed in bacteria. The amino acid sequences of nine selected members from this group were compared with that of SF173 (Figure 2a). Although the structure and molecular function of the UPF0253 members are unknown, we found an interesting annotation that one member of this family (a protein from *Gilliamella apicola*; UniProt ID A0A080LJU3) shares a Ta0600-like domain. Based on the SCOP database [22], the Ta0600-like superfamily belongs to a class of proteins with all  $\alpha$ -conformations and is assumed to have bromodomain-like folds composed of four-helix bundles. All of the three available Ta0600-like protein structures in PDB (2FU2, 2Q5b, and 2QZG) showed the four-helix bundle conformation (Figure S4). Although SF173 has no significant sequence similarity with these proteins, a structural comparison indicated that the central architecture of the SF173 dimer had a similar topology (Figure 2b). The interchain four-helix ( $\alpha 2$ ,  $\alpha 3$ ,  $\alpha 2'$ , and  $\alpha 3'$ ) bundle of SF173 could be well superimposed on the 2FU2, 2Q5B, and 2QZG structures, with r.m.s.d. of 2.991 Å (80 residues matched), 2.690 Å (72 residues matched) and 2.948 Å (72 residues matched), respectively (Figure 2c). Among those, the 2FU2-corresponding protein Sp-PIP from *Streptococcus pyogenes* has been recently suggested to be a novel type of bacteriocin-like immunity protein [23]. Bacteriocins (colicins in gram-negative bacteria) are anti-bacterial proteinaceous toxins produced by bacteria to compete against other bacterial strains, while immunity proteins act as inhibitors of their own bacteriocins or colicins [24]. The colicin D immunity protein (PDB 1V74) with a four-helix bundle conformation resembled SF173 at a first glance. Nevertheless, precise structural comparison excluded a significant structural homology, as the r.m.s.d. between SF173 and 1V74 structures is over 8.7 Å (data not shown).

Additionally, we investigated the operon correlation of SF173 with an expectation of finding meaningful relationships with immunity proteins. Colicin gene clusters are usually found on plasmids and commonly consist of three tightly linked genes encoding the toxin, immunity, and lysis proteins. In contrast, SF173 gene clusters are contained in genomic DNA, with the SF5M90T\_172 (SF172) and SF5M90T\_174 (SF174) loci located upstream and downstream of SF5M90T\_173 (SF173), respectively (Figure 3a). An analysis of bioinformatic databases revealed that the sf173-neighboring gene products, SF172 and SF174, are classified

as putative members of protein groups not related to the colicin-immunity protein system. All these results imply that SF173 is not likely related to the colicin immunity proteins, in spite of the structural similarities observed from the central four-helix bundle conformation. Meanwhile, the operon-related protein SF172 provided alternative clues for another putative function of SF173.

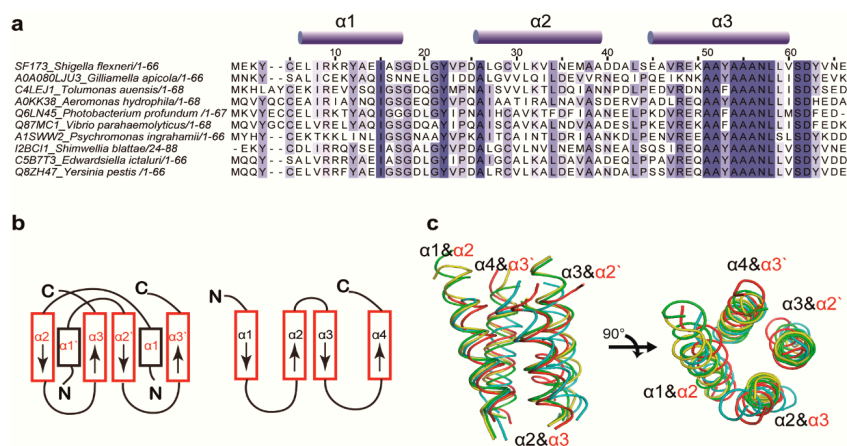


**Figure 2.** Structural similarity between TA0600-like domain proteins. (a) Multiple sequence alignment of homologous proteins in the UPF0253 family. Residue numbers and helix positions are presented for the SF173 sequence. Conserved residues are highlighted in blue, and the color intensity is proportional to the conservation score; (b) Comparison of the topology diagrams of the SF173 (left panel) and UPF0147-family protein (right panel) structures; (c) Structural superposition of SF173 (red) and UPF0147-family proteins (PDB ID 2QZG, yellow; 2FU2, cyan; 2QSB, green) in the four-helix bundle scaffold. The labels of the secondary structure of UPF0147-family and SF173 proteins are colored black and red, respectively.

### 3.3. Structural Correlation with ROF/RNase P-Like Domain Proteins

The InterPro analysis predicted that SF172, the upstream gene product of SF173, belongs to the ROF (modulator of Rho-dependent transcription termination) family of proteins sharing a Rof/RNase P-like domain. SF174, the downstream gene product of SF173, was annotated as an uncharacterized protein homologous to RfaH—a transcription elongation protein. In particular, the *sf172* and *sf173* genes share 14 bp nucleotides (Figure 3a), implying a close functional relationship, similar to the genetic overlapping frequently observed in bacterial toxin/anti-toxin systems [25,26]. Thus, the subsequent database search was focused on the ROF/RNase P-domain proteins. In particular, a PDB search for SF172 homologues found the solution structure of the YaeO protein from *E. Coli* (PDB ID 1SG5), which has 99% sequence identity to SF172. The *sf172-sf173-sf174* gene cluster in *S. flexneri* has an organization highly homologous to that of the *yaeO-yaeP-yaeQ* gene cluster in *E. coli* (Figure 3a). Thus, YaeP (98.5% sequence identity to SF173) and YaeQ (100% sequence identity to SF174) could also be identified as SF173 and SF174 orthologues, respectively. Although the structure and function of YaeP and YaeQ proteins are uncharacterized, YaeO has been identified as a Rho-specific inhibitor of transcription termination [27]. Bacteria have two major mechanisms for transcription termination, one of which is dependent on the transcription terminator protein Rho. YaeO can bind to Rho and act as a competitive inhibitor of RNA binding (Figure 3b).

Further inspection of ROF/RNase P-domain proteins suggested a possible correlation with SF173. The solution structure of RPP29 protein in the RPP29:RPP21 complex (PDB ID 2KI7) where RPP21 structure was listed in the result of a DALI search for SF173 structure, albeit with a low Z-score, has a structural similarity to ROF/RNase P-domain proteins including YaeO. As shown in Figure 4a, the local fold composed of  $\alpha 2$  and  $\alpha 3$  matches well (r.m.s.d. of 1.919 Å for 40 residues) with the two-helix region of the RPP21 part of the complex. RPP29 and RPP21 correspond to ribonuclease (RNase) P protein component 1 and 4, respectively, from *Pyrococcus furiosus*. RNase P is an RNA-based

ribozyme and its protein components are different among bacteria (one small protein), archaea (four or five different protein subunits) and eukaryotes (ten different protein components) [28]. As the product of locus SF5M90T\_3722 in the *S. flexneri* strain M90T is relevant to the sole protein component of the RNase P holoenzyme, SF172 and SF173 are not likely involved in the RNase P system. However, RNase P component proteins and ROF proteins appear to be closely related in terms of molecular evolution, as they are commonly associated with tRNA inhibition and share similar structural domains. In this context, it was noted that YaeO and RPP29 share a significantly similar structural topology and show a partial structural homology (structural superposition with r.m.s.d. of 4.560 Å for 64 residues; Figure 4b). The aforementioned genetic overlap in the SF172-SF173 genes and the fact that YaeO (SF172 orthologue) and SF173 structures resembled RPP29 and RPP21, respectively, suggested the formation of a SF172-SF173, as observed in the RPP29:RPP21 complex.

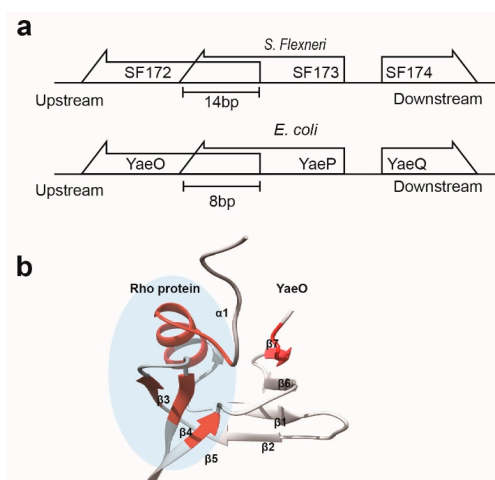


**Figure 3.** Structure and molecular interaction of SF172/YaeO (a) Schematic diagram showing gene arrangements in the sf172/yaeO-containing operons; (b) Ribbon presentation of the YaeO structure (PDB ID 1SG5), where the Rho-binding sites are colored red. Note that the complex structure is not available, and the binding site was determined by NMR spectroscopy [15].

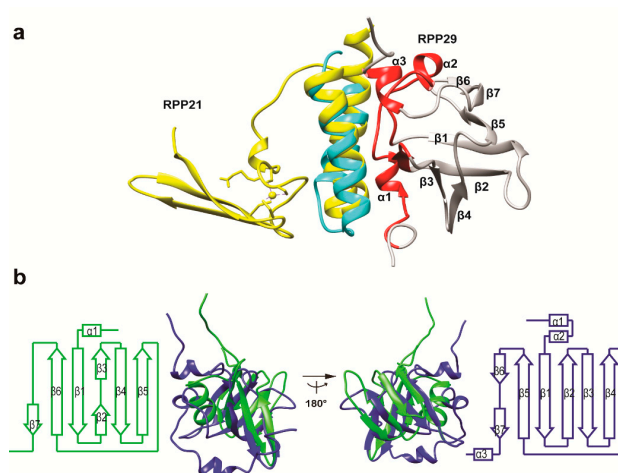


**Figure 4.** Structural comparison of the RPP21-RPP29 and SF173-YaeO (SF172) systems. (a) Ribbon presentation of the RPP21:RPP22 complex structure (PDB ID 2KI7). RPP21 and RPP29 are colored yellow and gray, respectively. The RPP21-binding site in RPP29 is highlighted in red. The region from  $\alpha 2$  to  $\alpha 3$  of the SF173 structure (cyan) was well superimposed onto the  $\alpha 1$  to  $\alpha 2$  region in the RPP21 structure; (b) Structural homology between YaeO (green) and RPP29 (blue). 3D structures were superimposed and topology diagrams are presented separately.

#### 4. Conclusions

The crystal structure of a functionally uncharacterized protein, SF173, was solved as a part of a structural genomics study on an important human pathogen *S. flexneri*. The structure was characterized as a helical bundle dimeric conformation with three  $\alpha$ -helices in each monomer. Bioinformatic analysis suggested that SF173 is also likely involved in the regulation of Rho-specific transcription termination, by binding to SF172/YaeO to inhibit interaction with Rho, in respect that the SF172 orthologue YaeO is a direct inhibitor of the bacterial transcription terminator Rho protein. Considering that the Rho-specific transcription termination system constitutes an essential and unique cellular process to bacterial species, a detailed understanding on the Rho-related proteins could provide a validated target for novel antibiotic development. Hence, a biological study to elucidate the physiological relevance of the putative molecular function of SF173 is currently in progress. In addition, our structural inspection, which indicated a partial structural homology of SF173 to colicin D and RPP21, implies a possible long-distance correlation in terms of genomic evolution among the bacteriocin/colicin-immunity, Rho-dependent transcription termination, and RNase P systems, all of which are associated with tRNA utilization [27,29,30].

**Supplementary Materials:** The following are available online at [www.mdpi.com/xxx/s1](http://www.mdpi.com/xxx/s1). Table S1: Summary of data collection and refinement statistics; Figure S1:  $2F_o - F_c$  electron density map of SF173 (contoured at 1.0 $\sigma$ ); Figure S2: Positions of conserved residues in the SF173 structure; Figure S3: Interchain electrostatic interactions in the SF173 structure; Figure S4: Structural homology of SF173.

**Acknowledgments:** This work was supported by grants of the Basic Science Research Program through the National Research Foundation (NRF) of Korea, funded by the Ministry of Education, Science and Technology (2017R1A2B1006357) and the Korea Health Technology R&D Project through the Korea Health Industry Development Institute (KHIDI), funded by the Ministry of Health & Welfare, Republic of Korea (grant number: HI17C0927).

**Author Contributions:** Ji-Hun Kim, Hyung-Sik Won, and Min-Duk Seo conceived and designed the experiments; Won-Su Yoon, Seung-Hyeon Seok, Bong-Jun Jung and Seu-Na Lee performed the experiments; Ji-Hun Kim, Seung-Hyeon Seok and Dae-Won Sim analyzed the data; Hyung-Sik Won and Min-Duk Seo contributed reagents/materials/analysis tools; Ji-Hun Kim, Hyung-Sik Won, and Min-Duk Seo wrote the paper. All authors reviewed the manuscript.

**Conflicts of Interest:** The authors declare no conflict of interest.

#### References

1. Drews, J. Drug discovery: A historical perspective. *Science* **2000**, *287*, 1960–1964. [CrossRef] [PubMed]
2. Grabowski, M.; Chruszcz, M.; Zimmerman, M.D.; Kirillova, O.; Minor, W. Benefits of structural genomics for drug discovery research. *Infect. Disord. Drug Targets* **2009**, *9*, 459–474. [CrossRef] [PubMed]
3. Sansonetti, P.J. Microbes and microbial toxins: Paradigms for microbial-mucosal interactions III. Shigellosis: From symptoms to molecular pathogenesis. *Am. J. Physiol. Gastrointest. Liver Physiol.* **2001**, *280*, G319–G323. [CrossRef] [PubMed]
4. Perdomo, O.J.; Cavaillon, J.M.; Huerre, M.; Ohayon, H.; Gounon, P.; Sansonetti, P.J. Acute inflammation causes epithelial invasion and mucosal destruction in experimental shigellosis. *J. Exp. Med.* **1994**, *180*, 1307–1319. [CrossRef] [PubMed]
5. Kotloff, K.L.; Winickoff, J.P.; Ivanoff, B.; Clemens, J.D.; Swerdlow, D.L.; Sansonetti, P.J.; Adak, G.K.; Levine, M.M. Global burden of Shigella infections: Implications for vaccine development and implementation of control strategies. *Bull. World Health Organ.* **1999**, *77*, 651–666. [PubMed]
6. Hale, T.L. Genetic basis of virulence in Shigella species. *Microbiol. Rev.* **1991**, *55*, 206–224. [PubMed]
7. Jin, Q.; Yuan, Z.; Xu, J.; Wang, Y.; Shen, Y.; Lu, W.; Wang, J.; Liu, H.; Yang, J.; Yang, F.; et al. Genome sequence of Shigella flexneri 2a: Insights into pathogenicity through comparison with genomes of Escherichia coli K12 and O157. *Nucleic Acids Res.* **2002**, *30*, 4432–4441. [CrossRef] [PubMed]
8. Onodera, N.T.; Ryu, J.; Durbic, T.; Nislow, C.; Archibald, J.M.; Rohde, J.R. Genome sequence of Shigella flexneri serotype 5a strain M90T Sm. *J. Bacteriol.* **2012**, *194*, 3022. [CrossRef] [PubMed]
9. Ashkenazi, S.; Levy, I.; Kazaronovski, V.; Samra, Z. Growing antimicrobial resistance of Shigella isolates. *J. Antimicrob. Chemother.* **2003**, *51*, 427–429. [CrossRef] [PubMed]
10. Sansonetti, P.J. Shigellosis: An old disease in new clothes? *PLoS Med.* **2006**, *3*, e354. [CrossRef] [PubMed]

11. Simmons, K.J.; Chopra, I.; Fishwick, C.W. Structure-based discovery of antibacterial drugs. *Nat. Rev. Microbiol.* **2010**, *8*, 501–510. [[CrossRef](#)] [[PubMed](#)]
12. Kim, H.N.; An, J.G.; Lee, Y.S.; Seok, S.H.; Yoo, H.S.; Seo, M.D. Overexpression, purification, crystallization and preliminary X-ray crystallographic analysis of SF173 from *Shigella flexneri*. *Acta Crystallogr. F Struct. Biol. Commun.* **2015**, *71*, 54–56. [[CrossRef](#)] [[PubMed](#)]
13. Jancarik, J.; Scott, W.G.; Milligan, D.L.; Koshland, D.E., Jr.; Kim, S.H. Crystallization and preliminary X-ray diffraction study of the ligand-binding domain of the bacterial chemotaxis-mediating aspartate receptor of *Salmonella typhimurium*. *J. Mol. Biol.* **1991**, *221*, 31–34. [[CrossRef](#)]
14. Otwinowski, Z.; Minor, W. Processing of X-ray diffraction data collected in oscillation mode. *Macromol. Crystallogr. Part A* **1997**, *276*, 307–326.
15. Hendrickson, W.A.; Teeter, M.M. Structure of the hydrophobic protein crambin determined directly from the anomalous scattering of sulphur. *Nature* **1981**, *290*, 107–113. [[CrossRef](#)] [[PubMed](#)]
16. Terwilliger, T.C.; Adams, P.D.; Read, R.J.; McCoy, A.J.; Moriarty, N.W.; Grosse-Kunstleve, R.W.; Afonine, P.V.; Zwart, P.H.; Hung, L.-W. Decision-making in structure solution using Bayesian estimates of map quality: The PHENIX AutoSol wizard. *Acta Crystallogr. D Biol. Crystallogr.* **2009**, *65*, 582–601. [[CrossRef](#)] [[PubMed](#)]
17. Adams, P.D.; Afonine, P.V.; Bunkoczi, G.; Chen, V.B.; Davis, I.W.; Echols, N.; Headd, J.J.; Hung, L.W.; Kapral, G.J.; Grosse-Kunstleve, R.W.; et al. PHENIX: A comprehensive Python-based system for macromolecular structure solution. *Acta Crystallogr. D Biol. Crystallogr.* **2010**, *66*, 213–221. [[CrossRef](#)] [[PubMed](#)]
18. Emsley, P.; Lohkamp, B.; Scott, W.G.; Cowtan, K. Features and development of Coot. *Acta Crystallogr. D Biol. Crystallogr.* **2010**, *66*, 486–501. [[CrossRef](#)] [[PubMed](#)]
19. Walther, D.; Eisenhaber, F.; Argos, P. Principles of helix-helix packing in proteins: The helical lattice superposition model. *J. Mol. Biol.* **1996**, *255*, 536–553. [[CrossRef](#)] [[PubMed](#)]
20. Holm, L.; Park, J. DaliLite workbench for protein structure comparison. *Bioinformatics* **2000**, *16*, 566–567. [[CrossRef](#)] [[PubMed](#)]
21. Mitchell, A.; Chang, H.Y.; Daugherty, L.; Fraser, M.; Hunter, S.; Lopez, R.; McAnulla, C.; McMennamin, C.; Nuka, G.; Pesseat, S.; et al. The InterPro protein families database: The classification resource after 15 years. *Nucleic Acids Res.* **2015**, *43*, D213–D221. [[CrossRef](#)] [[PubMed](#)]
22. Murzin, A.G.; Brenner, S.E.; Hubbard, T.; Chothia, C. SCOP: A structural classification of proteins database for the investigation of sequences and structures. *J. Mol. Biol.* **1995**, *247*, 536–540. [[CrossRef](#)]
23. Chang, C.; Coggill, P.; Bateman, A.; Finn, R.D.; Cymborowski, M.; Otwinowski, Z.; Minor, W.; Volkart, L.; Joachimiak, A. The structure of pyogenecin immunity protein, a novel bacteriocin-like immunity protein from *Streptococcus pyogenes*. *BMC Struct. Biol.* **2009**, *9*, 75. [[CrossRef](#)] [[PubMed](#)]
24. Chavan, M.A.; Riley, M.A. Molecular evolution of bacteriocins in Gram-negative bacteria. In *Bacteriocins*; Springer: Berlin, Germany, 2007; pp. 19–43.
25. Han, K.D.; Matsuura, A.; Ahn, H.C.; Kwon, A.R.; Min, Y.H.; Park, H.J.; Won, H.S.; Park, S.J.; Kim, D.Y.; Lee, B.J. Functional identification of toxin-antitoxin molecules from *Helicobacter pylori* 26695 and structural elucidation of the molecular interactions. *J. Biol. Chem.* **2011**, *286*, 4842–4853. [[CrossRef](#)] [[PubMed](#)]
26. Kwon, A.R.; Kim, J.H.; Park, S.J.; Lee, K.Y.; Min, Y.H.; Im, H.; Lee, I.; Lee, B.J. Structural and biochemical characterization of HP0315 from *Helicobacter pylori* as a VapD protein with an endoribonuclease activity. *Nucleic Acids Res.* **2012**, *40*, 4216–4228. [[CrossRef](#)] [[PubMed](#)]
27. Gutierrez, P.; Kozlov, G.; Gabrielli, L.; Elias, D.; Osborne, M.J.; Gallouzi, I.E.; Gehring, K. Solution structure of YaeO, a Rho-specific inhibitor of transcription termination. *J. Biol. Chem.* **2007**, *282*, 23348–23353. [[CrossRef](#)] [[PubMed](#)]
28. Hartmann, E.; Hartmann, R.K. The enigma of ribonuclease P evolution. *Trends Genet. TIG* **2003**, *19*, 561–569. [[CrossRef](#)] [[PubMed](#)]
29. Graille, M.; Mora, L.; Buckingham, R.H.; van Tilbeurgh, H.; de Zamaroczy, M. Structural inhibition of the colicin D tRNase by the tRNA-mimicking immunity protein. *EMBO J.* **2004**, *23*, 1474–1482. [[CrossRef](#)] [[PubMed](#)]
30. Holzmann, J.; Frank, P.; Löffler, E.; Bennett, K.L.; Gerner, C.; Rossmann, W. RNase P without RNA: Identification and functional reconstitution of the human mitochondrial tRNA processing enzyme. *Cell* **2008**, *135*, 462–474. [[CrossRef](#)] [[PubMed](#)]

